SIXTH FRAMEWORK PROGRAMME
EURATOM
Management of Radioactive Waste

Project acronym:	EUROTRANS
Project full title:	EUROpean Research Programme for the TRANSmutation of High Level Nuclear Waste in an Accelerator Driven System
Contract no.:	FI6W-CT-2004-516520

Domain:	*DM1 DESIGN*
Workpackage N°:	*WP 1.3 ACCELERATOR*
Identification N°:	*D 1.3.14*
Type of document:	*Deliverable*
Title:	*Beam dynamics calculations for fault-tolerance*
Dissemination Level:	*CO*
Reference:	*EUROTRANS / D 1.3.14, Revision 0*
Status:	*Final*

	Name	Partner	Date	Signature
written by: (*)	J-L. Biarrotte D. Uriot	CNRS CEA	25/10/2007	
Task leader: (*)	J-L. Biarrotte	CNRS	25/10/2007	
WP leader: (*)	A.C. Mueller	CNRS	25/10/2007	
DM leader: (*)				
IP leader: (*)				

(*) when relevant

SIXTH FRAMEWORK PROGRAMME

IP-EUROTRANS
- INTEGRATED PROJECT ON EUROPEAN TRANSMUTATION -

BEAM DYNAMICS CALCULATIONS FOR FAULT-TOLERANCE

Jean-Luc Biarrotte, CNRS, IPN Orsay,
Didier Uriot, CEA Saclay.

Document date: Monday, 29 October 2007

1 INTRODUCTION

The European Transmutation Demonstration requires a high-power proton accelerator operating in CW mode, ranging from 1.5 MW (XT-ADS operation, @ 600 MeV) up to 16 MW (EFIT, @ 800 MeV). A reference design for this accelerator is being developed since 2001 through the PDS-XADS and the EUROTRANS programmes [e.g. 1,2,3,4]; it is mainly based on the use of a superconducting linac, from at least 20 MeV. Such a choice allows to obtain a very modular and upgradeable machine (same concept for prototype and industrial scale), an excellent potential for reliability, and a high RF-to-beam efficiency thanks to superconductivity (optimized operation cost).

The ADS accelerator is also expected – especially in the long term EFIT scenario – to have a very limited number of unexpected beam interruptions per year, which would cause the absence of the beam on the spallation target for times longer than one second. This requirement is motivated by the fact that frequently repeated beam interruptions induce thermal stresses and fatigue on the reactor structures, the target or the fuel elements, with possible significant damages, especially on the fuel claddings; moreover these beam interruptions decrease the plant availability, implying plant shut-downs in most of the cases. Therefore, it has been estimated that beam trips in excess of one second duration should not occur more frequently than five times per 3-month operation period for the XT-ADS, and three times per year for the EFIT.

To reach such an ambitious goal, which is lower than the reliability experience of typical accelerator based user facilities by 2 or 3 orders of magnitude, it is clear that reliability-oriented design practices need to be followed from the early stage of components design. In particular:

- "strong design" practices are needed: every linac main component has to be de-rated with respect to its technological limitation (over-design);
- a rather high degree of redundancy needs to be planned in critical areas; this is especially true for the identified "poor-reliability" components: linac injector, and RF power systems, where solid-state amplifiers should be used as much as possible;
- fault-tolerance capabilities have to be introduced to the maximum extent: such a capability is expected in the highly modular superconducting RF linac [5].

The goal of this document is precisely to investigate in more details the fault-tolerance capability of the XT-ADS linac.

2 SUPERCONDUCTING LINAC & FAULT-TOLERANCE

2.1 The XT-ADS reference superconducting linac

In the present XT-ADS linac reference scheme, a fully modular superconducting linac, based on the use of independently-phased RF structures (spoke, elliptical), accelerates the beam from "X MeV" up to the final energy (600 MeV). This "X MeV" energy, which corresponds to the transition between the redundant injector and the fault-tolerant superconducting linac, is still to be optimized between 5 and 50 MeV. It will be definitely frozen, probably around 17 MeV, at the end of the EUROTRANS programme, together with a new optimized linac design for the XT-ADS reference accelerator.

Table 1 presents, from the PDS-XADS study, a possible layout for the modular superconducting linac, starting from X = 5 MeV. This particular accelerator scheme, which corresponds to the largest energy range possible for the independently-phased section, will be used to perform the fault-tolerant analysis. The reference optical design is shown on Figure 1. More details on this design can be found in [1].

Table 1 – General layout of a 5 – 600 MeV XT-ADS linac using only independently phased SC cavities.

Section number	**1**	**2**	**3**	**4**	**5**
Input Energy [MeV]	5	16.7	90.5	191.7	498.1
Output Energy [MeV]	16.7	90.5	191.7	498.1	614.7
Cavity Technology	Spoke 352.2 MHz		Elliptical 704.4 MHz		
Structure β	0.15	0.35	0.47	0.65	0.85
Number of cavity cells	2	2	5	5	6
Number of cavities	36	60	28	51	12
Focusing type	NC quadrupole doublet				
Cavities/Lattice	2	3	2	3	4
Synch Phase [deg]	-40 to -27	-27 to -20	-25		
Lattice length [m]	1.58	2.42	4.16	5.73	8.37
Section Length [m]	28.5	49.0	58.5	98.5	26
<gradient> [MeV/m]	0.4	1.5	1.7	3.1	4.5

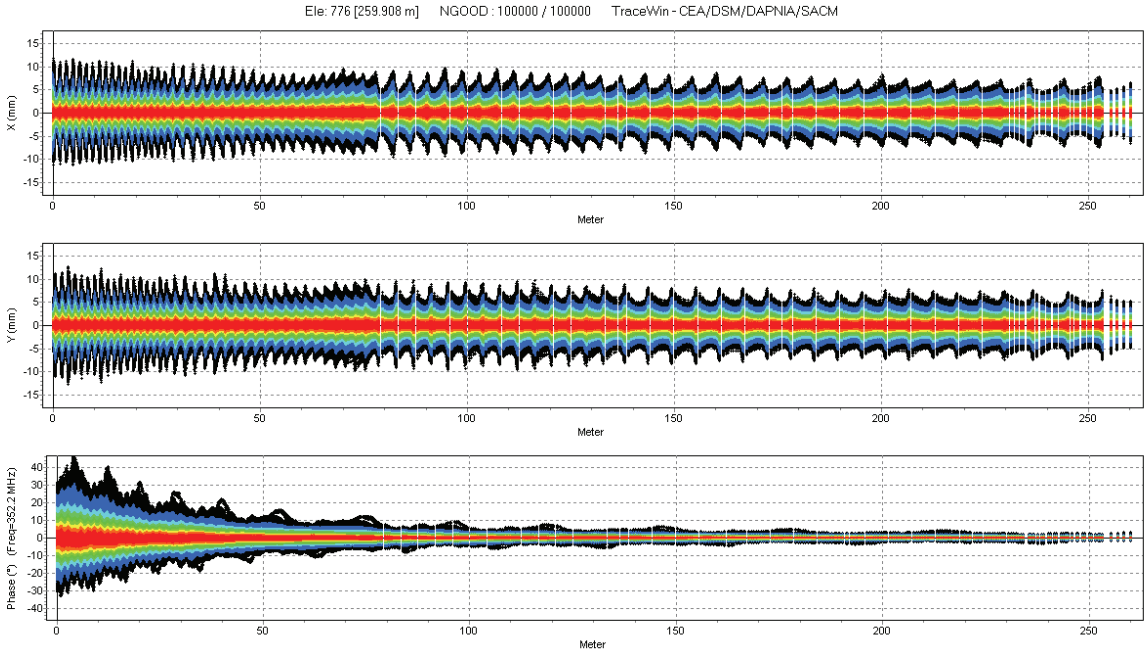

Figure 1 – Nominal beam envelopes in the 5 – 600 MeV XT-ADS linac (multi-particle simulation).

2.2 The fault-tolerance strategy

During the PDS-XADS project, systematic beam dynamics simulations in the stationary regime have already been performed on this reference accelerator to analyze the consequences of a cavity (or RF power system) failure [1,5]. From this first analysis, it appears that if nothing is done, a cavity's failure leads in nearly all the cases to a complete beam loss, due to the non-relativistic varying velocity of the particles. To avoid such a total beam loss, it is clear that some kind of retuning has to be performed to compensate the lack of acceleration due to the faulty cavity.

To achieve this compensation, the general philosophy is to re-adjust the accelerating fields and phases of the non-faulty accelerating cavities to recover the nominal beam characteristics at the end of the linac, and in particular its energy, while ensuring the same level of transmission than in the reference linac case. This is a "global feedback" concept (see Figure 2). This can be done using all the cavities downstream the faulty cavity ("general compensation method"), or only using the accelerating cavities neighbouring the failing one ("local compensation method"). In both cases, the retuning procedure, to be fast enough, requires some fast longitudinal beam dynamics simulations and/or the use of a predefined set-points database before being performed. Indeed, relying on longitudinal beam diagnostics (phase detectors, time of flight), as depicted in the ideal feedback scheme of Figure 2, appears to be far too long to apply in practice.

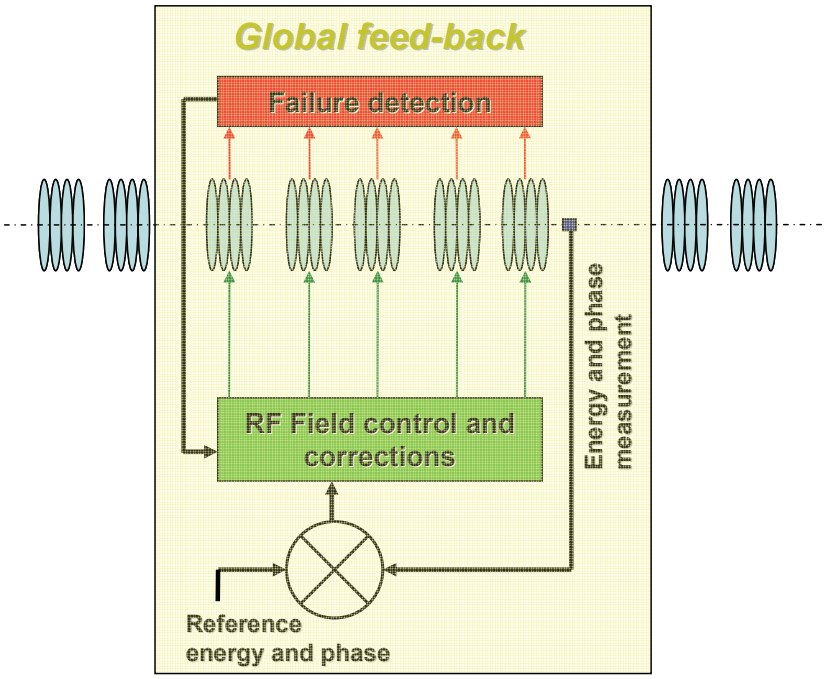

Figure 2 – Global feedback scheme for RF-fault recovery procedures.

In the general compensation method, all the linac components downstream the faulty cavity are retuned, so that the over-power required to compensate the faulty element is shared between a large number of RF cavities: the clear advantage is that this method only requires very few margins in terms of RF power and accelerating field. But this statement is only valid if the retuning is performed one single time; in order to recover several faulty situations (it is a priori our case), the RF margins have to be increased to roughly the same level as in the "local compensation method". On the other hand, the global retuning procedures become more complex than the local one, since involving a high number of elements, and the probability for retuning errors might be higher. On the practical point of view, a very important step has already been reached since this method has been demonstrated on-line at the SNS, where such a fault-recovery system has been recently tested on real operation with low average current high-velocity proton beams (>200MeV) [6]. The time required to achieve such a retuning is about a few minutes presently, but could probably be lowered to a few seconds or even less than a second [7]. Of course, during the retuning procedure, the beam has to be stopped.

The local compensation method, on the contrary, has the advantage of involving a small number of elements, simplifying the retuning procedures and limiting the possible induced errors. It is illustrated on Figure 3: if cavity #n is faulty, the 4 surrounding cavities (#n-2, #n-1, #n+1, #n+2) are retuned to recover the nominal beam energy & phase at the end of the following lattice (point M), and by consequence, at the linac end. It can of course be done with more (or less) cavities if necessary. Beam dynamics simulations show that the nominal beam parameters at the target can always be restored using such a retuning method, even if the cavity failure happens at very low energy, given the condition that a +30% rise in RF power and accelerating field can be sustained in the cavities [5]. It has to be noted nevertheless that the situation is substantially more difficult to manage in the low energy

section of the linac (below 20 MeV and even more below 10 MeV), due to the very low velocity of the beam, and consequently to its still quite high non-normalized (geometrical) longitudinal emittance: in this low-energy case, one has also to take care in the retuning procedure not only of the beam phase and energy, but also of its longitudinal phase advance. The local compensation method is of course demanding in terms of RF power budget, but it is in-line with the ADS over-design criterion, so that it should not lead to dramatic over-costs.

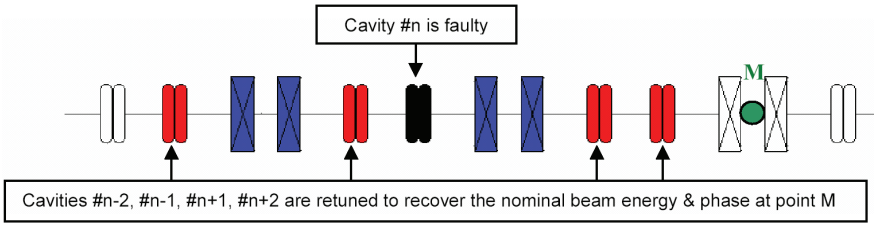

Figure 3 – Principle of the local compensation method.

From the previous statements, it appears that some kind of compromise should be found concerning the number of cavities to be use in the recovery procedures. This "optimal" number will have to be searched for, relying especially on a detailed global reliability analysis of the XT-ADS machine, planned to be performed in 2008 / 2009, and on practical experimental results later on. But in any case, the retuning philosophy remains the same.

2.3 Investigating fast failure recovery scenarios

The remaining step in the fault-tolerance analysis is now to identify and develop fast failure recovery scenarios to ensure that such retunings can be performed in less than 1 second. Two ways are investigated.

The first way is to stop the beam to achieve the retuning (Scenario n°1). This solution is compatible with both general and local compensation methods, and is already used at the SNS (but with "minutes" beam stops up to now). On the beam dynamics point of view, it has already been demonstrated in the previous PDS-XADS studies dedicated to the stationary fault-tolerance analysis, as mentioned before. This method would probably require practically:

In less than 1 sec

- fast fault detection and beam shut-down;
- fast access to a predefined set-point general database, or to the result of an appropriated longitudinal beam dynamics fast simulation;
- fast update and tracking of the new LLRF field and phase set-points;
- adequate management of the tuner of the failed cavity to put it off frequency and avoid any deceleration effect due to beam loading;
- beam re-injection.

The other way is to try to perform the retuning without stopping the beam (Scenario n°2). This solution, which is a priori more compatible with the local compensation method (minimisation of the number of transient adjustments), has to be demonstrated on the beam dynamics point of view to check if it can cope with the probable induced transient beam losses. This transient study is actually the main topic of this note. In this case, the procedure would probably require practically:

Fast enough to avoid significant beam losses

- very fast fault detection;
- fast access to a predefined set-points general database;
- fast update and tracking of the new field and phase set-points, based on the foreseen failed cavity transient behaviour (pre-calculated tables), to recover quickly the nominal beam transmission and energy;
- slow update and tracking of the new field and phase set-points with the same method while detuning the failed cavity to avoid the beam loading effect;

Finally one has to note that in every scenario, digital techniques become necessary to meet the speed and software configuration required by such retuning procedures. FPGA-based digital LLRF control systems, in which a number of key functionalities are implemented on a single chip, can offer such a high-grade reliability and flexibility. Developments are going on in CEA and CNRS at 704 MHz and 352 MHz respectively in the frame of Task 1.3.4, with very encouraging preliminary results [8,9].

3 TRANSIENT BEHAVIOURS OF A RF CAVITY

In order to investigate precisely into Scenario n°2 (transient retuning procedure without stopping the beam), one has first to understand the transient behaviours of the accelerating RF cavities in the linac environment.

3.1 Modelling the RF cavity + beam

The spoke and elliptical RF superconducting cavities operate with the $TM_{010-\pi}$ mode, which produces an accelerating RF voltage on the cavity axis. Using the RLC circuit analogy, the behaviour of the "cavity + beam" system can be described at first order by the following equation [10]:

$$(1) \qquad \frac{d\tilde{V}_C(t)}{dt} = \frac{\omega\,(r/Q)}{4}\left(2\tilde{I}_G(t) + \tilde{I}_B(t)\right) - \frac{\omega\,(1 - j\tan\psi(t))}{2\,Q_L}\tilde{V}_C(t)$$

$\tilde{V}_C$ represents the low frequency component of the accelerating voltage created in the cavity at the operating RF frequency $\omega = 2\pi f$. Its amplitude $V_C = \left|\tilde{V}_C\right| \approx \left|\int E_Z(z)\, e^{j\omega z/\beta c} dz\right|$ gives the voltage seen by a particle, with velocity β and optimal phase, while crossing the cavity (the Transit Time Factor is included). Its phase $\varphi_C = \arg(\tilde{V}_C)$ gives the phase of this accelerating voltage, compared to the reference phase of the system which is chosen here to be the phase giving a 0° synchronous phase. In the case where the cavities are modelled using punctual gaps, this phase is therefore directly equal to the synchronous phase.

$\tilde{I}_B$ represents the low frequency component of the beam current crossing the cavity. For short bunches, its amplitude is given by $I_B = \left|\tilde{I}_B\right| \approx 2\,I_0$, where I_0 is the beam mean current. Its phase $\varphi_B = \arg(\tilde{I}_B) = \pi$ by definition of the reference phase.

$\tilde{I}_G$ represents the low frequency component of the current created by the RF power generator. Its amplitude is given by $I_G = \left|\tilde{I}_G\right| = 2\sqrt{P_{inc}/((r/Q)\,Q_i)}$, where P_{inc} is the incident RF power, (r/Q) the cavity shunt impedance (linac definition), and Q_i the incident coupling. Its phase is noted $\varphi_G = \arg(\tilde{I}_G)$.

The resonant frequency of the cavity f_{cav} is always varying because of various perturbations (microphonics, Lorentz detuning…), and these perturbations can not be neglected because of the thin bandwidth of the loaded cavity. These fluctuations are included

in (1) through the detuning angle of the cavity $\tan\psi(t) \cong 2Q_L\,(f_{cav}(t) - f)/f$, where Q_L is the quality factor of the loaded cavity ($1/Q_L = 1/Q_0 + 1/Q_i + 1/Q_t$). We choose to describe these frequency fluctuations with a first order model using the following equation (2), where $\Delta f_{CTS}(t)$, $\Delta f_L(t)$, $\sum_i \Delta f_{MIC_i}(t)\sin(2\pi f_{MIC_i} t)$ are the detuning contributions from cold tuning system management, Lorentz forces, and microphonics respectively, k_L is the Lorentz force detuning coefficient in Hz/(MV/m)^2, and τ_m is the mechanical time constant of the cavity.

$$(2) \qquad f_{cav}(t) = f + \Delta f_L(t) + \Delta f_{CTS}(t) + \sum_i \Delta f_{MIC_i}(t)\sin(2\pi f_{MIC_i} t) \text{ with } \frac{d\,\Delta f_L(t)}{dt} = \frac{1}{\tau_m}\left(\frac{10^{-12} k_L}{L_{acc}^{\,2}} V_C^{\,2}(t) - \Delta f_L(t)\right)$$

The resolution of the coupled equations (1) and (2) gives the transient evolution of the accelerating voltage $\tilde{V}_C(t)$ in the cavity. More details can be found in [11].

3.2 Modelling the RF regulation loop

Due to various perturbations (cavity frequency variations, beam transients…), the accelerating voltage $\tilde{V}_C(t)$ produced in the cavity from (1) + (2) is not stable at all. In order to regulate the accelerating field and phase, a regulation loop is required, called "Low-level RF" (LLRF) regulation loop. Its role is to monitor the field produced in the cavity using a capacitive probe, perform an adequate treatment of the signal, compare it to the desired (V_C, φ_C) set-point, and use the detected error to react on the RF high-power amplifier stage via a PID (Proportional / Integrative / Derivative) controller.

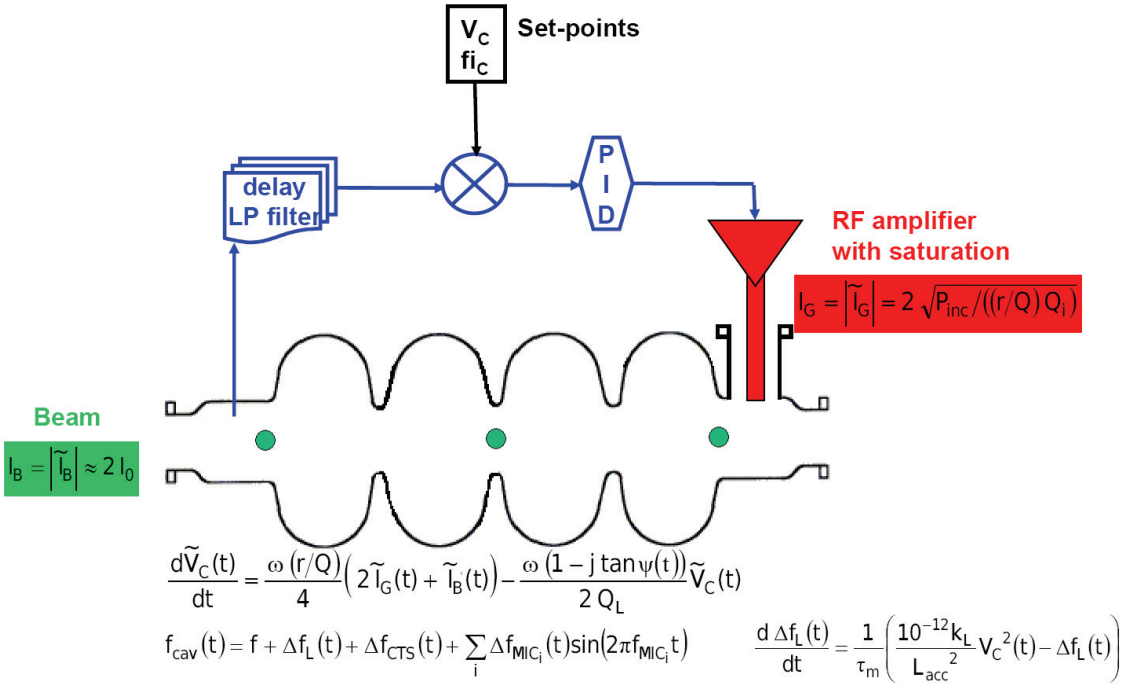

Figure 4 – Modelling of an accelerating RF cavity and its associated RF control loop.

A rough but meaningful modelling of such a loop has been defined, illustrated in Figure 4. The main elements are:

- a comparator that monitors the probe signal and compare it to the desired set-point; at this location of the loop, the signals have been digitalized, and the comparison is made using I/Q signals (see [8,11] for more details);
- a PID controller (we will here only use the gain "P" as a first approach);
- a delay or/and a low-pass filter to account for the bandwidth of the whole system; the typical order of magnitude is a few μs delays, and a few kHZ cut-off frequency.

3.3 A few RF cavity behaviours

The figures below illustrate RF cavity behaviours in a few situations. Calculations are made for a beta 0.35 Spoke cavity with optimal coupling and detuning angle. The main parameters can be found in Table 2. Microphonics, Lorentz force detuning are taken into account, such as amplifier saturation and loop delay; the simulation always starts in an already stationary regime.

- Figure 5 shows the case where the cavity is loaded with a 10 mA CW beam, and fed at constant RF power (around 15 kW) without any RF regulation loop: dramatic field and phase instabilities are recorded, mainly due to microphonics fluctuations.
- Figure 6shows the same case, but with the RF regulation loop operating with a gain of 20: the RF input power is thus adapting itself to provide excellent field and phase stability.
- Figure 7shows the case of the system reaction to a 0-current beam hole of 200 μs with loop gain of 60: the field and phase stability remains very good, within the specifications ($<\pm1\%$, $<\pm1°$).
- Finally, Figure 8 shows the case where the RF input power is suddenly shut down (RF failure), while the beam is still on: the beam loading effect is observed, and the cavity then develops decelerating fields.

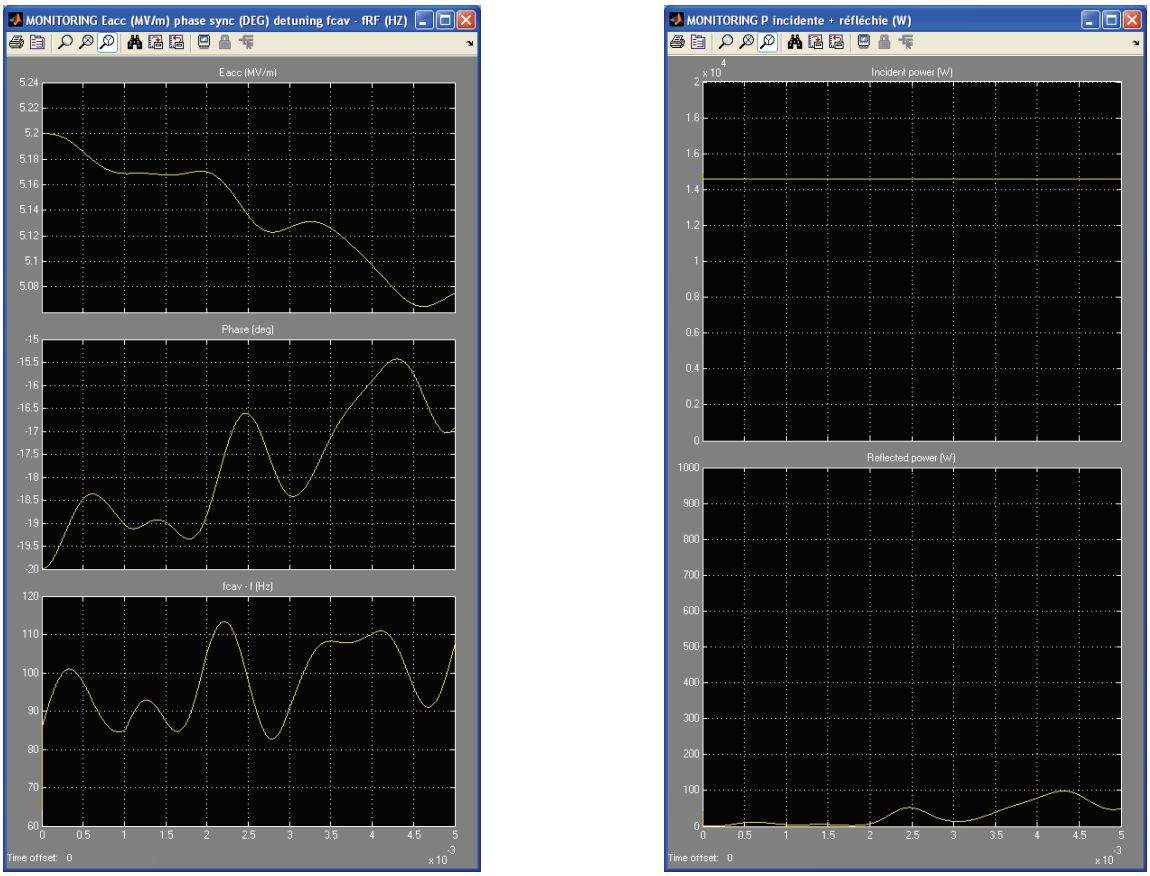

Figure 5 : RF control loop opened

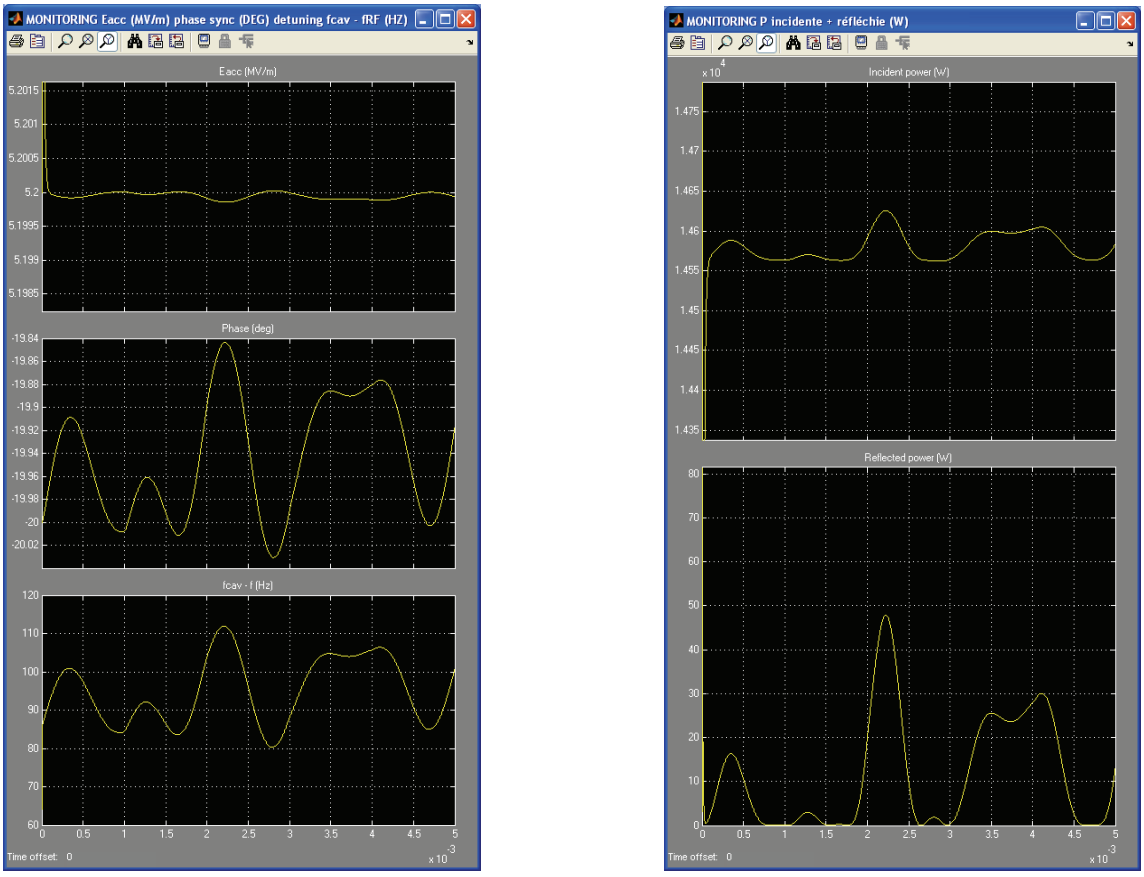

Figure 6 : RF control loop closed

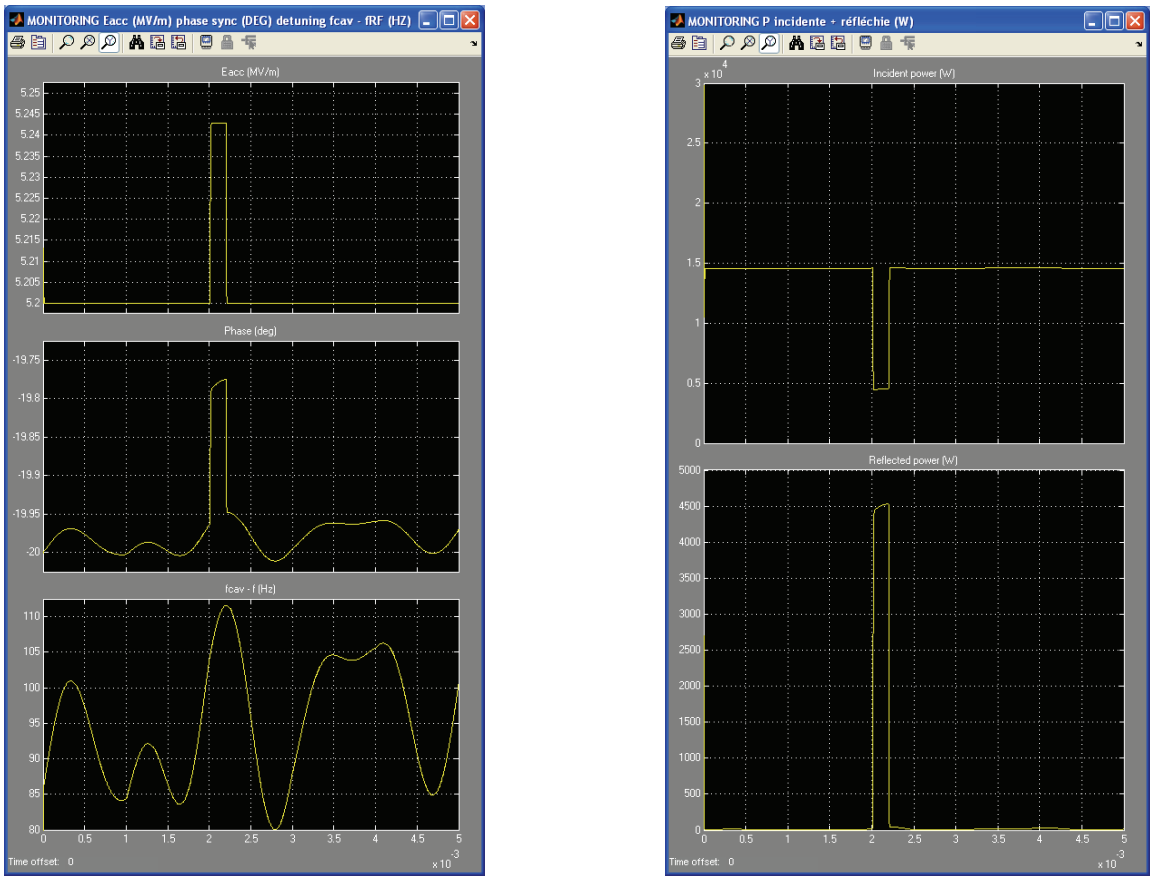

Figure 7 : Beam hole

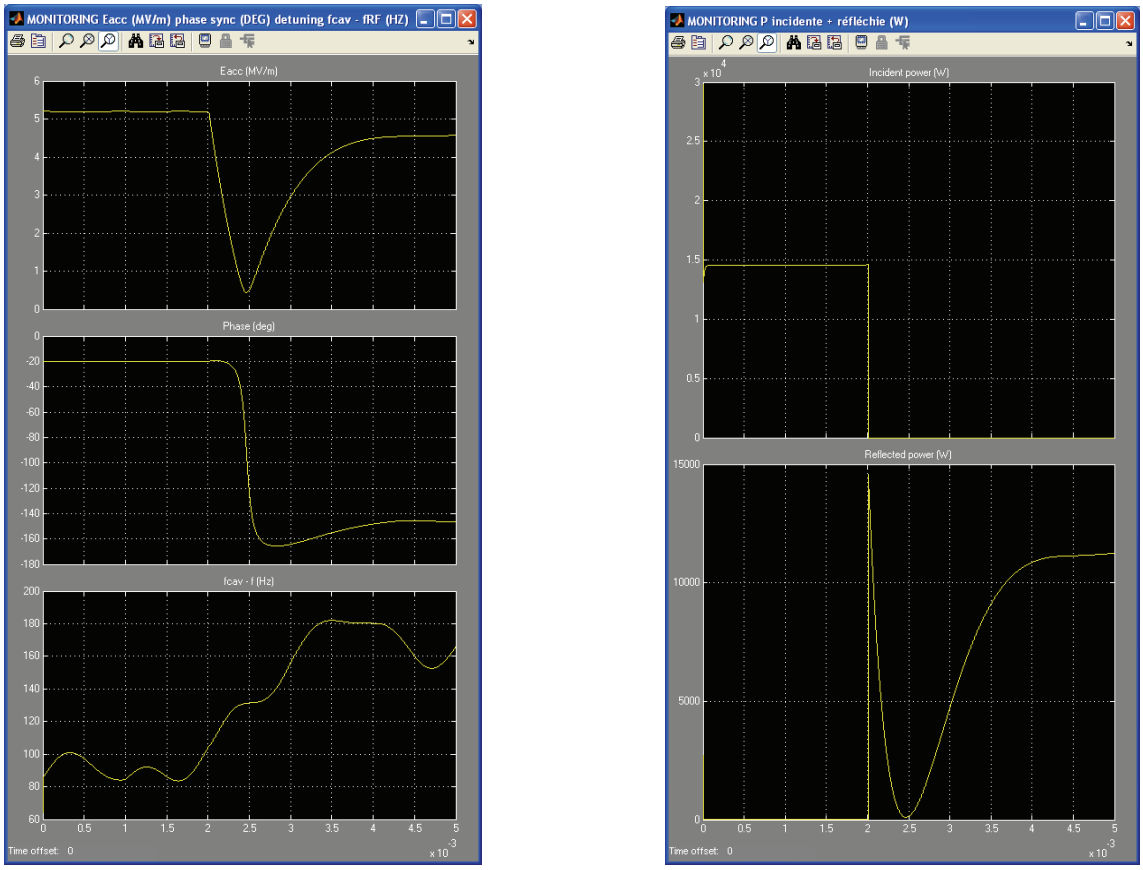

Figure 8 : RF failure

4 COUPLING RF AND BEAM DYNAMICS

In order to test the global feed-back scheme within Scenario n°2 (local compensation method with no beam stop), a new tool was needed in order to better understand the beam transients behaviours during RF cavity faults, and the right way to recover the correct energy output. The objective was here to develop a tool able to simulate the transient states of a full linac, each accelerating cavity using its own RF control loop. This has been done coupling the cavity model shown in the preceding chapter with a beam transport code including space-charge capability and high level cavity description based on multi-gap model or field map elements.

4.1 Simulation code development

The cavity model describing the transient RF cavity behaviour has first been included into the beam envelope and multiparticle CEA code TraceWin [12]. Successful validation tests have been performed to compare the results produced by this new cavity module with previous Simulink results.

The TraceWin code is in charge to transport the reference particle of the machine (envelope) or the beam distribution (multiparticle) through the cavities of the linac, and is by default a "static" tool. It has thus been modified to be able to include the "time" variable, and therefore perform simulations at different times. The architecture of the TraceWin code "transient calculation" option is shown in Figure 9. Several time steps are involved in the process. From the initial condition, at t=0, where all the cavities are set to their nominal RF fields and phases, different time-based iterations are performed:

- every δt_0 (time integration step), a new couple of RF field amplitude and phase is evaluated in each cavity of the linac according to RF cavity model;
- every δt_1 (time envelope step, $\delta t_1 \geq \delta t_0$), a new beam transport calculation is performed through the linac (envelope transport), using the RF field characteristics (amplitude and phase) obtained at this time in each cavity (which can be modelled either by multi-gap or field map element); this calculation updates the beam characteristics at each linac location;
- every δt_2 (time multiparticle step, $\delta t_2 \geq \delta t_1$), a multiparticle transport simulation is performed; this calculation updates the beam characteristics at each linac location;
- every δt_3 (time storage step, $\delta t_3 \geq \delta t_2$), all the linac and beam characteristics at each location are stored.

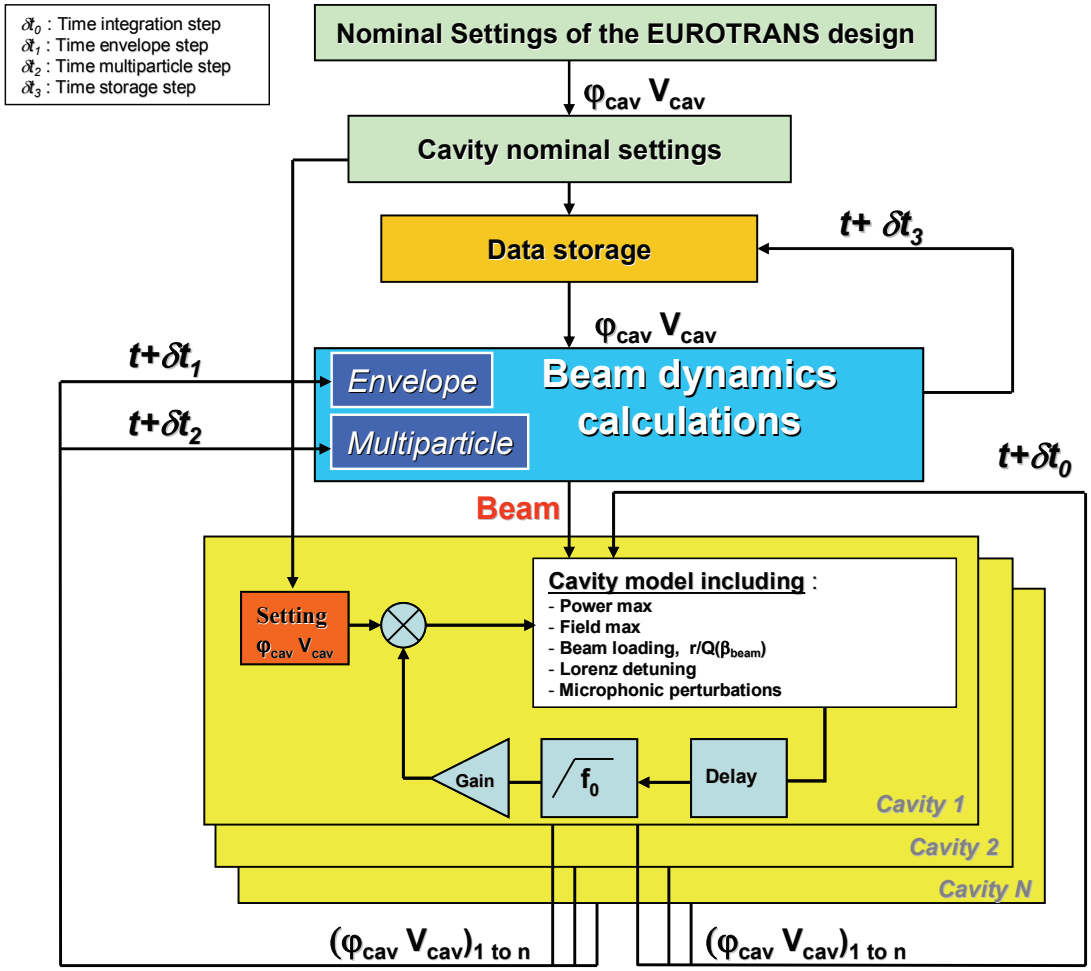

Figure 9 – Code architecture.

Obviously, the computation time strongly depends on the choice of these different time steps, and especially on δt_1 and δt_2; δt_3 is fixed by the available memory. Typically, to simulate accurately a 10 ms linac behaviour, the time steps are respectively chosen to δt_0=1 ns, δt_1=1 µs, δt_2=10 µs and δt_3=10 µs. With 10 000 macro-particles, about 1 Gb memory is needed to save the results, and the simulation spends about 22 hours on a usual PC.

Finally, let's note that for each kind of cavity of the linac, a file has to be created in order to indicate to the transport code its main characteristics. These files have to contain also the feedback loop parameters, which can be different according to the cavity type. All these data are summarized in Table 2 in the case of our XT-ADS reference linac. Some extra parameters as microphonic frequencies and amplitudes can be added if needed.

Table 2 – Cavity and RF loop characteristics used for XT-ADS linac transient calculations.

	Spoke β=0.15	Spoke β=0.35	Elliptic β=0.47	Elliptic β=0.65	Elliptic β=0.85
RF power at saturation (kW)	15	30	80	150	150
Accelerating field margin (%)	50	50	50	50	50
r/Q at optimal beta (Ω)	101	220	153	316	598
Form factor (Ω)	72	101	101	194	300
Lorenz factor (Hz/(MV/m)^2)	-8	-8	-8	-8	-2
Feed-back delay (s)	2 10^{-6}	2 10^{-6}	2 10^{-6}	2 10^{-6}	2 10^{-6}
Feed-back gain	20	20	100	100	100
Low filter frequency (kHz)	10	10	10	10	10
Cryogenic operating T (K)	4.2	4.2	2	2	2

4.2 Code capabilities

Obviously, this new simulation code, which is a quite unique tool, potentially allows performing a lot of different studies on the linac response to various transient phenomenons: influence of microphonics, LLRF feed-back quality in presence of beam hole, etc…

Figure 10 and Figure 11 show for example the output energy of the first and last cavity of the EUROTRANS linac in the case where 3 microphonic fluctuations (100Hz, 600Hz and 1000Hz) of different amplitudes are present in the linac cavities (RF control loop on). Only the microphonic phases are randomly set. The red curve called "Linac" represents the reference "static" case, and the blue one called "Beam" represents the "transient" case (here: with microphonics)*.

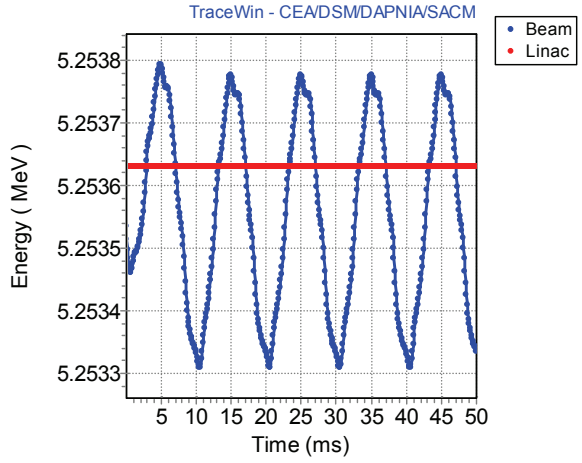

Figure 10 – Output energy of the first linac cavity with microphonics perturbations.

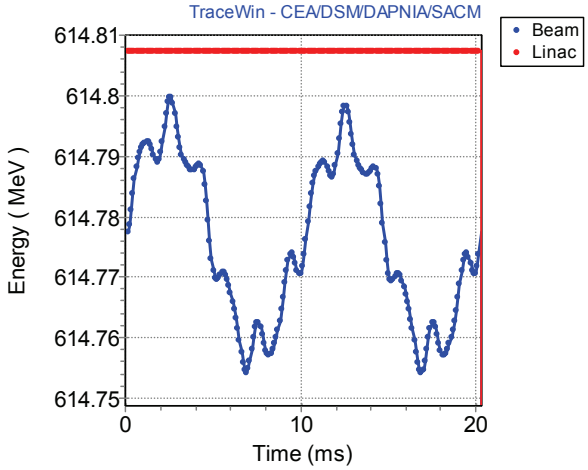

Figure 11 – Output energy of the last linac cavity with microphonics perturbations.

* In the full following document, all the charts will always show these two curves: red = static case; blue = transient case (i.e. with cavity failure).

Within the present study, this new tool will be used to analyse, on the beam dynamics point of view, the feasibility of a cavity-fault recovery procedure without stopping the beam (Scenario n°2). To this respect, the global feed-back scheme has been of course also implemented in the code. It is based on the same concept that the one used in our preceding "static" fault-tolerance analysis [5]: a few lattices downstream the faulty cavity, the beam energy and phase are monitored, and the cavities surrounding the failed one are retuned (fields and phases corrections are optimized via iterative calculations) to recover the nominal beam energy and phase at the monitoring location. The only difference is that, in this new transient study, the field and phase correction is not performed one single time per fault condition, like in the "static" case, but for each time step δt_2.

5 RF CAVITY FAULT: SIMULATION RESULTS

The goal here is not to study all the cases of cavity fault, but just to demonstrate a concept. For this reason, the analyse of the fast cavity-fault recovery procedure without stopping the beam (Scenario n°2) is performed for the following case: failure of Spoke cavity #92 (β=0.35) located near the end of the second linac section. The considered beam current is 10 mA, corresponding to a nominal ~15 kW to give to the beam. We will only concentrate on this specific case.

5.1 RF cavity failure without compensation

The goal here is to study the linac and beam behaviour when a cavity breaks down. All cavities are simulated with their feedback loop closed, and we consider the following timing:

- t = 0, all cavities of the linac are set at the nominal field and power. The energy output is stable according to time.
- t = 0+ε, ε being negligible, a RF cavity / amplifier breaks down (RF power off); the associated feedback loop is then opened.

The analysis of the beam behaviour in this case where nothing is done to recover the situation will help us to determine the time we have to react and perform the first compensations in order to conserve the beam with good parameters (emittances, energy, phase…).

The results are shown in the following figures. Figure 12 and Figure 13 show the transient evolution of the accelerating field and of the beam synchronous phase in the failed cavity. After about 500 µs, the field is coming close to 0, and after 2.5 ms the cavity becomes a decelerating cavity (see the fast phase shift), producing a decelerating field roughly equal to the nominal accelerating field. This is due to the beam loading effect, and it happens because we don't have the time in Scenario n°2 to detune the failed cavity to put if off frequency. This is a major difference with Scenario n°1, in which we can detune the cavity during the 1 second beam hole and avoid this decelerating effect at the beam reinjection.

The consequence to the output beam energy is shown on Figure 14, that shows the beam going out of the linac acceptance after about 240 µs. The final energy output is then stabilized around 90 MeV, which is already the beam energy at the failed cavity.

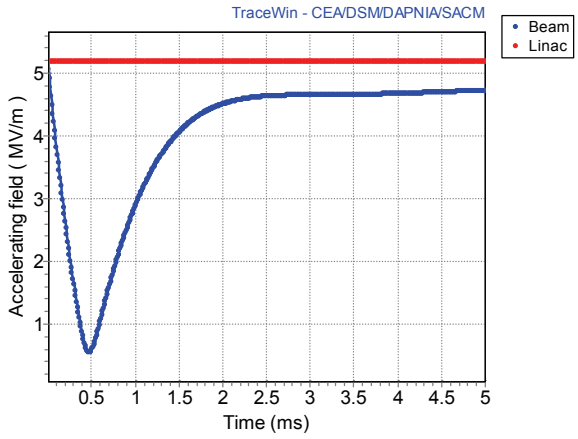

Figure 12 : Field in the failed cavity.

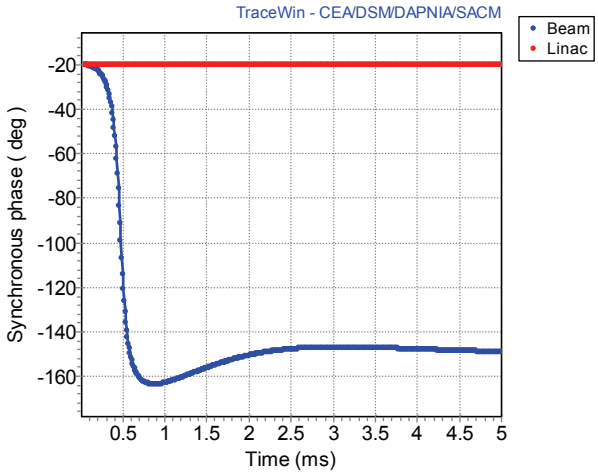

Figure 13 : Synchronous phase in the failed cavity

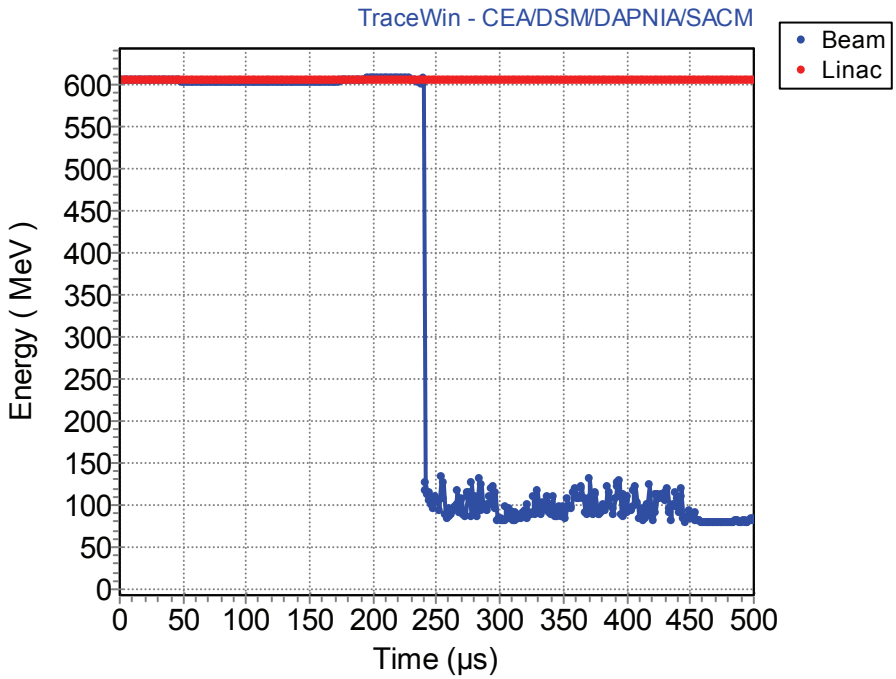

Figure 14 : Output beam energy at the linac end

The new tool also allows studying the beam transverse behaviour with respect to time. Figure 15 to Figure 18 illustrate for example the beam envelope at different times. Multi-particle simulations show that the first beam losses are observed after 160 µs (cf. Figure 19), and Figure 20 and Figure 21, plotted at 220 µs, show beam losses of about 33% distributed all along the linac end (failed cavity position is about 75 metres). We have to notice that TraceWin considers a particle as lost only when it reaches the beam tube (no cutt-off in energy or phase is used here).

These results mean that if we want to retune some cavities so as to keep the entire beam during the whole procedure, we will have to start it, in this specific case, 160 µs at maximum after the cavity failure.

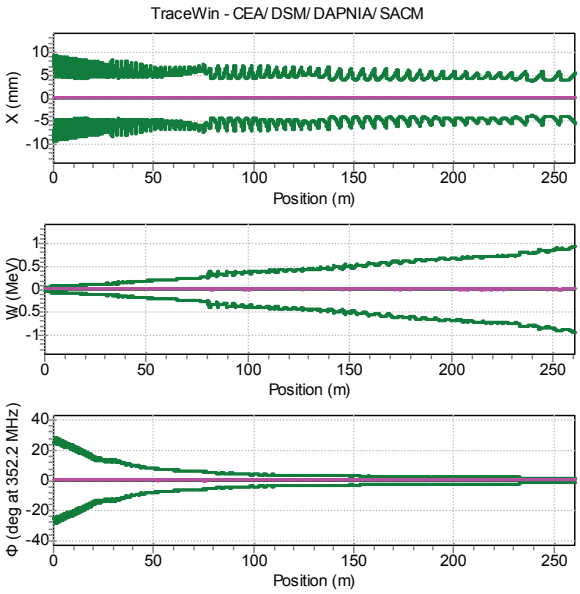

Figure 15 : Envelopes at 0 µs, reference linac

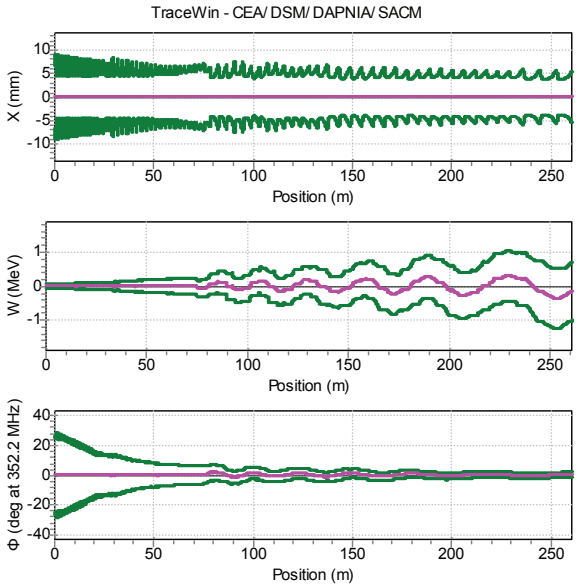

Figure 16 : Envelopes at 20 µs

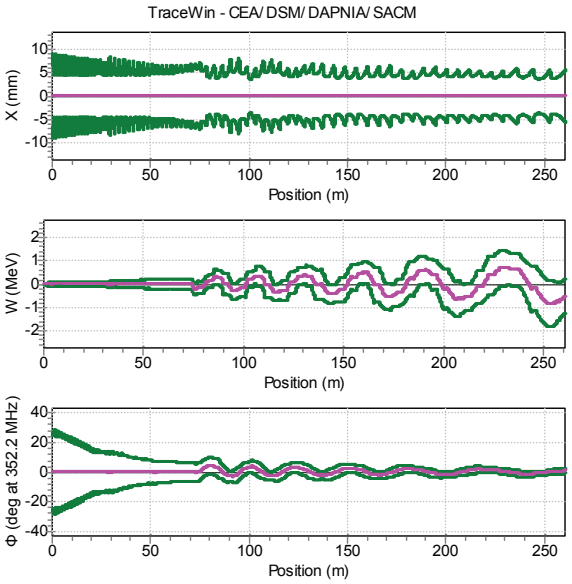

Figure 17 : Envelopes at 50 µs

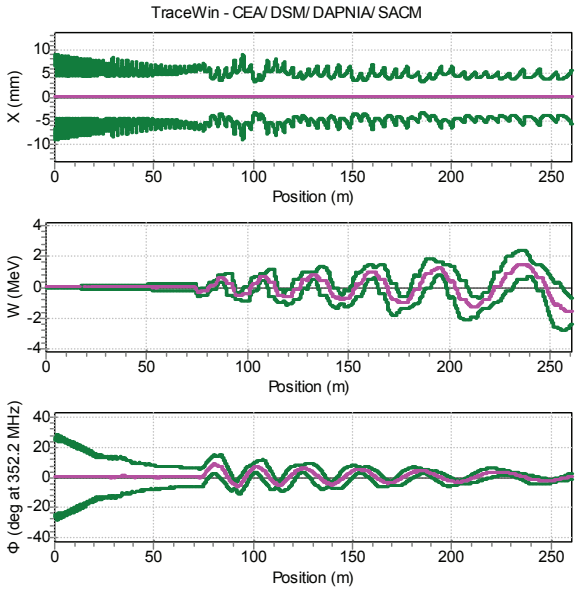

Figure 18 : Envelopes at 100 µs

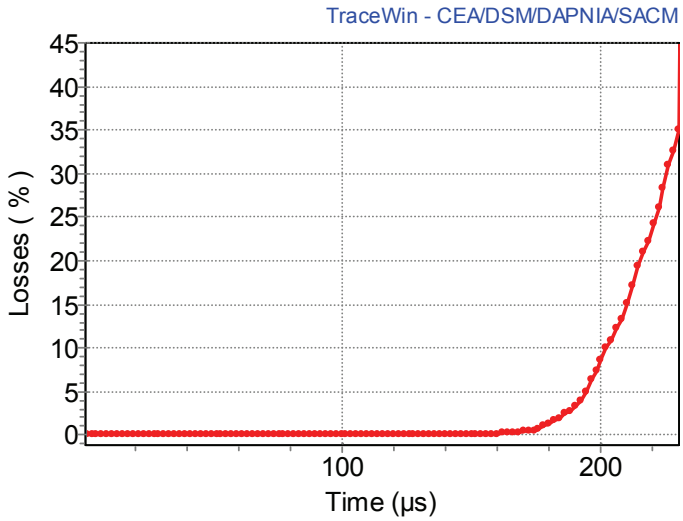

Figure 19 : Beam losses according to time

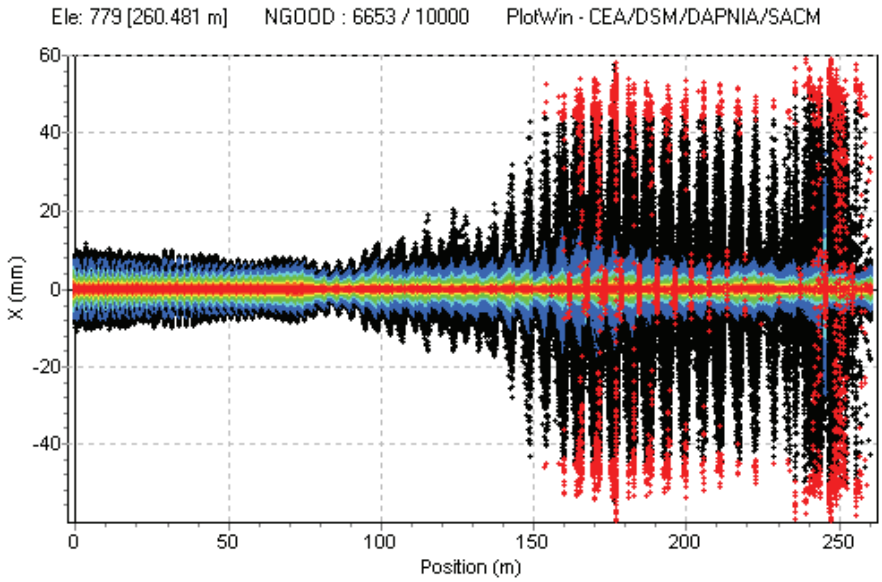

Figure 20 : Transverse beam distribution at 220 µs, in red are plotted the losses

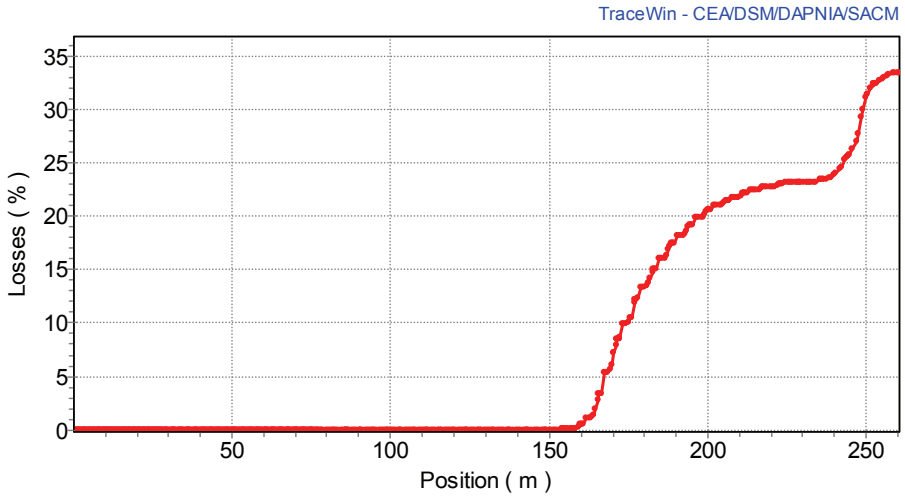

Figure 21 : Losses along the linac at 220 µs.

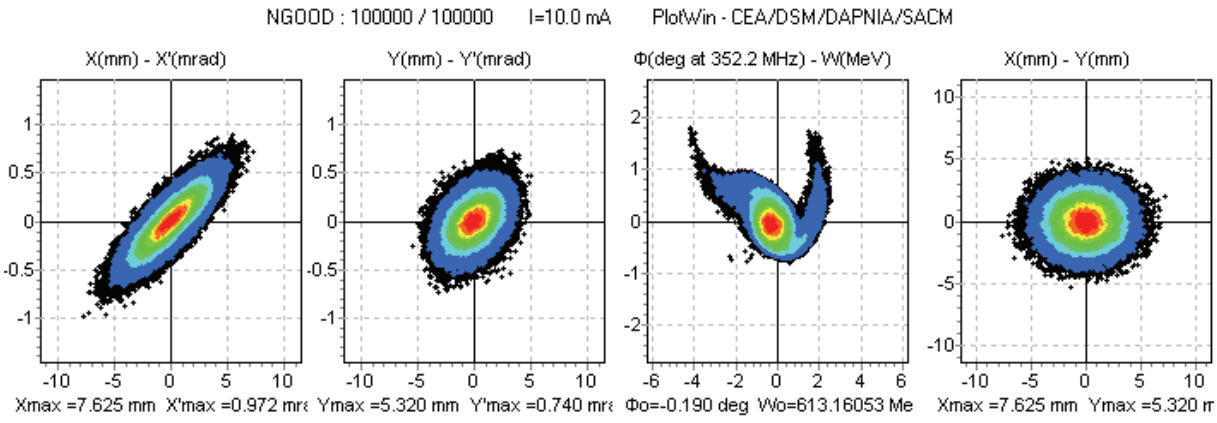

Figure 22 : Beam distributions output at 100µs.

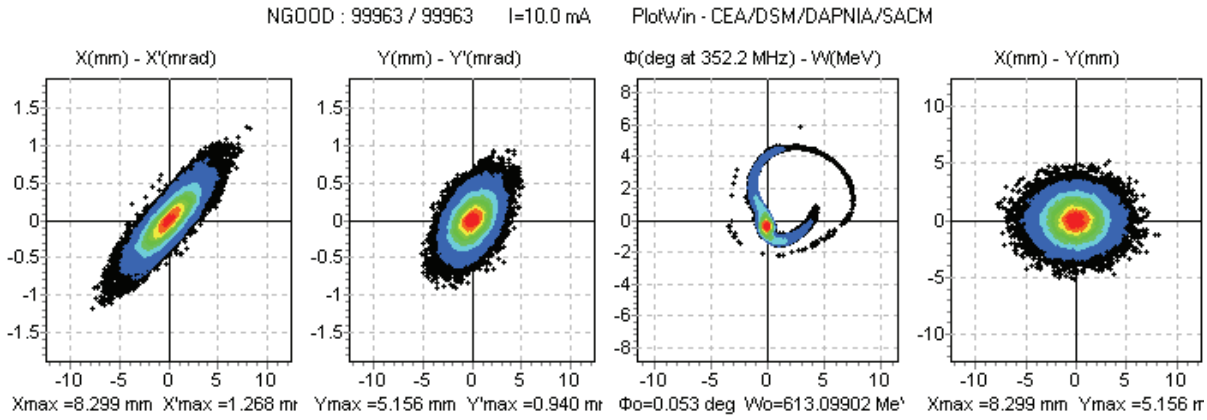

Figure 23 : Beam distributions output at 150µs, longitudinal émittance starts to increase.

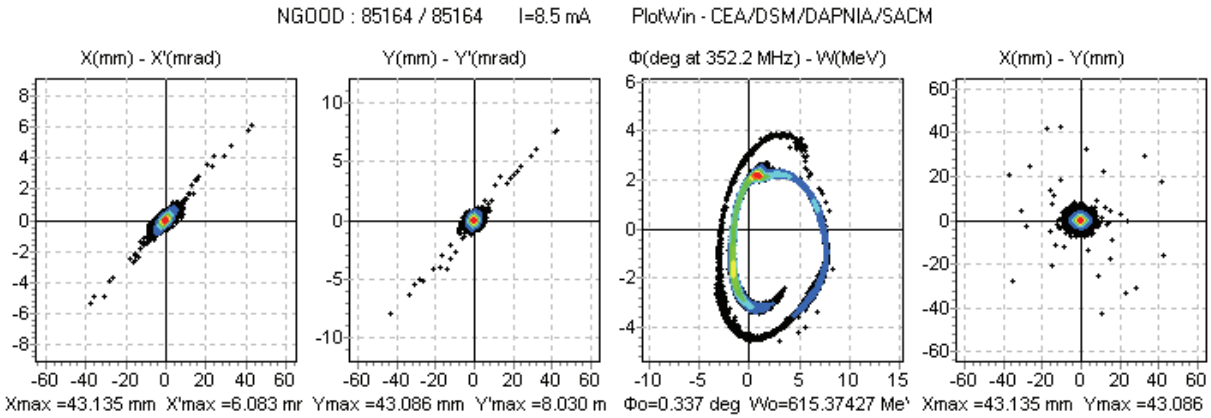

Figure 24 : Beam distributions output at 200µs, 10% of particle left linac acceptance.

5.2 RF cavity failure with compensation

The procedure to conserve the beam is based on the following timing:

- t = 0: the RF cavity / amplifier breaks down (RF power off); the associated feedback loop is then opened and the cavity field starts to decrease.
- $t = T_1$: first couples of set-points (V_C, φ_C) are sent to the adjacent cavities, computed from the situation at T_1. T_1 represents the time needed to detect the failure, and has to be short enough to conserve a correct beam transport.
- $t = T_1 + T_2$: second couples of set-points (V_C, φ_C) are sent to the adjacent cavities, computed from the situation at $T_1 + T_2$.
- Every T_2, new couples of set-points (V_C, φ_C) are sent to the adjacent cavities, until the beam behaviour becomes stable in phase and energy. T_2 has also to be short enough to conserve a correct beam transport.

In the simulation, at each T_2 step, couples of new set-points (V_C, φ_C) are estimated by an optimization obtained by iteration from the beam phase and energy monitoring. As already mentioned, for the real accelerator operation, these sets of retuning values will have to be pre-calculated by simulations, and store in a table in order to be able to be applied very quickly when needed. This means that, once the linac design frozen, each case of cavity failure will has to be study beforehand.

The results presented after are still given for the Spoke cavity #92 failure. Several cases have been looked at, with different numbers of correcting cavities, available power margins, accelerating field margins, or different T_1 and T_2. Only one case is presented in the following, corresponding to the following hypotheses:

- 30 kW RF amplifiers saturation level (see Table 2);
- 50 % accelerating field margin (see Table 2);
- 6 Spoke cavities (3 before + 3 after) used to compensate the cavity failure. If the accelerating field margin is reduced to 40 %, then 8 neighbouring cavities are needed.

As already discussed, the failed cavity is not detuned in this Scenario n°2, and thus produces a decelerator field due to the beam loading effect. This is why more cavities and/or margins are needed here than in Scenario n°1, in which less than 30 % field margins for the same retuning with 3+3 cavities, and ~25 kW amplifiers could be used in this section [5].

Given these parameters, it can be showed that a transient fault-recovery procedure without stopping the beam is manageable without any beam loss.

- 40 corrections have been calculated and set to neighbouring cavities during the whole retuning procedure.
- The final beam energy is recovered and stable after 3 ms (Figure 25). The maximum energy error is about 2.2 MeV at 140 μs, that gives a maximum power fluctuation at the target of 0.5%. At 140 μs, we also record the maximum beam synchronous phase error (5°) in the last cavity of the linac (Figure 26).
- Less than 10% of transverse emittance growth is observed (Figure 27), with no beam loss observed during the 3 ms of simulation with 10 000 macro-particles.
- The worse beam transport is at 140 μs. Figure 28 shows the output space phase beam at 140 μs and Figure 29 shows the emittance behaviour along the linac at this time. We clearly see the longitudinal emittance increasing, but the beam keep a correct transport allowing to get at the output only 10% transverse emittance growth.

Finally, the six last charts represent the field evolution in the six cavities used to compensate the failed cavity.

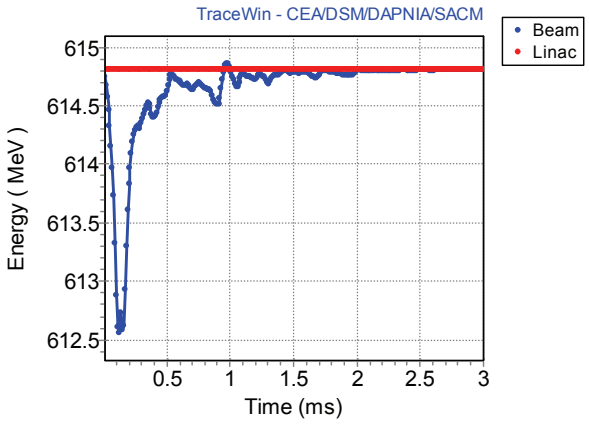

Figure 25 : Output beam energy

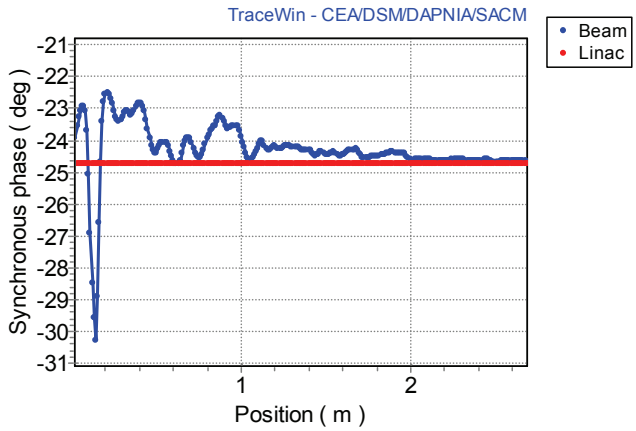

Figure 26 : Beam synchronous phase at last cavity

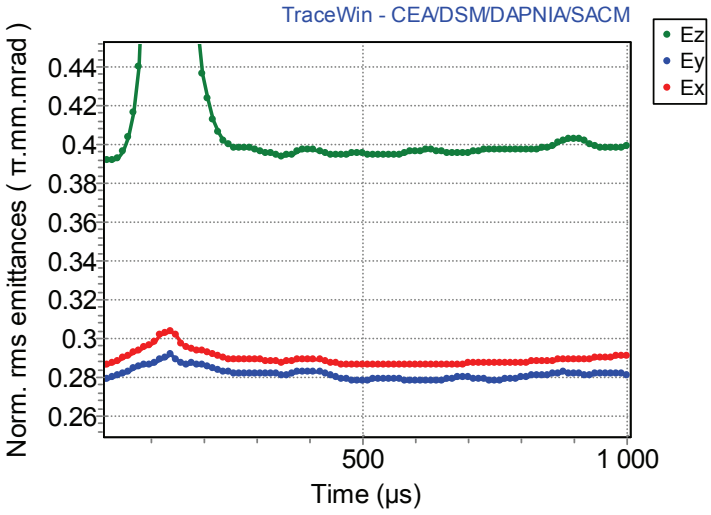

Figure 27 : Emittance evolution during the first ms

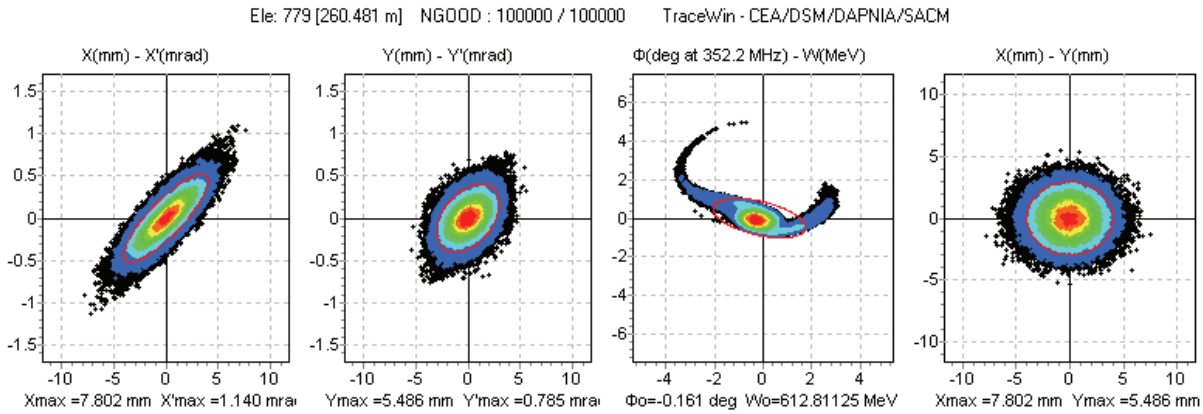

Figure 28 : Output beam phase spaces at 140 µs

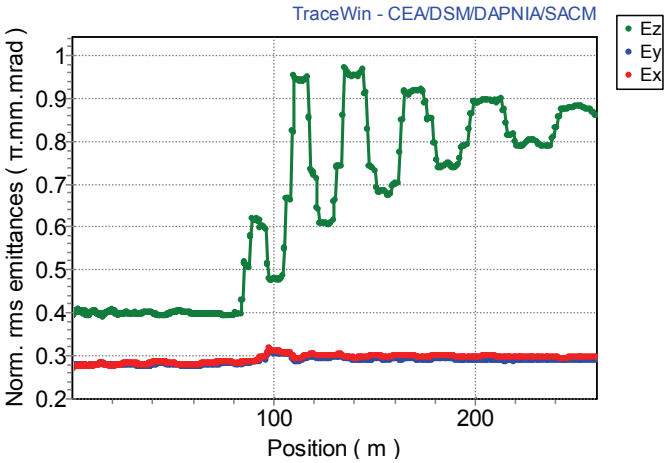

Figure 29 : Emittances along the linac at 140 µs

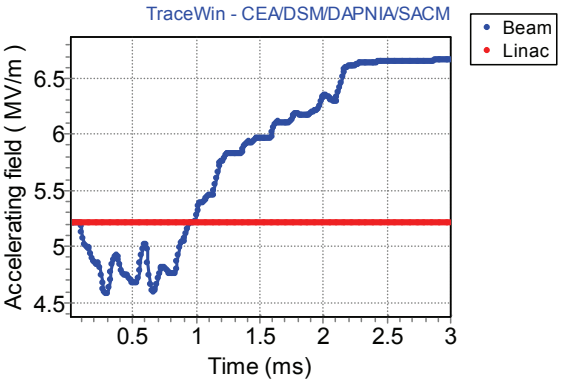

Figure 30 : Field in cavity #1

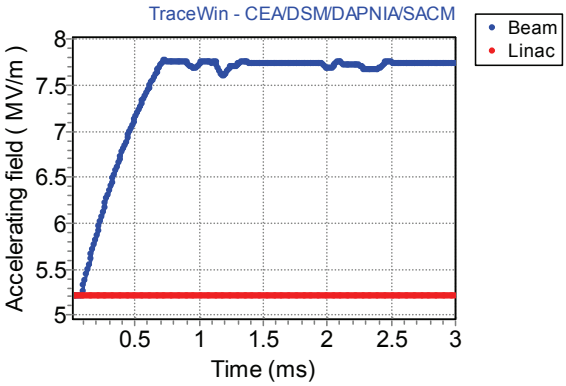

Figure 31 : Field in cavity #2

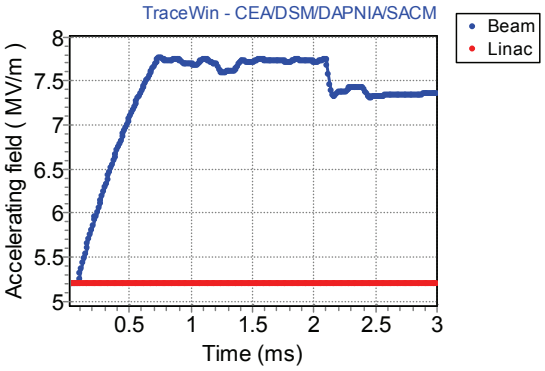

Figure 32 : Field in cavity #3

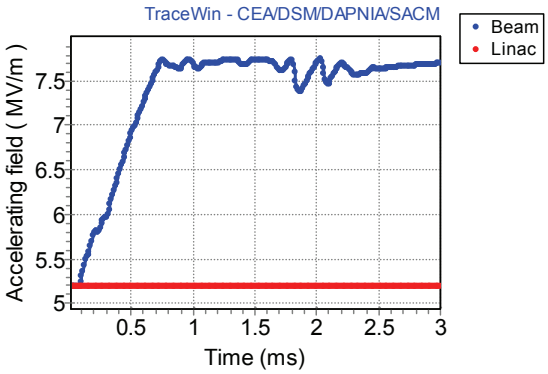

Figure 33 : Field in cavity #4

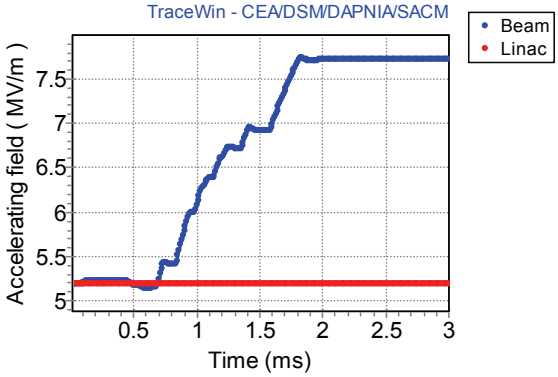

Figure 34 : Field in cavity #5

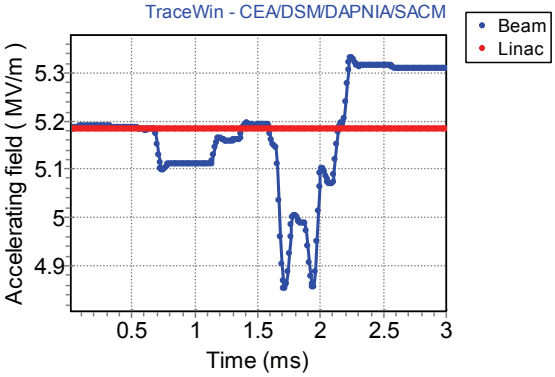

Figure 35 : Field in cavity #6

5.3 Time limits

In this specific, the time limit to start correction is 150 µs. If the compensation procedure starts later, the beam begins to get out the linac acceptance and beam losses appear. The correction step has to be smaller than 150 µs. In the example shown Figure 36, some beam losses are observed when the compensation starts at 200 µs. Note that this time limits strongly depends of the beam current. Higher is the beam current, faster the global feed-back system will have to start its corrections.

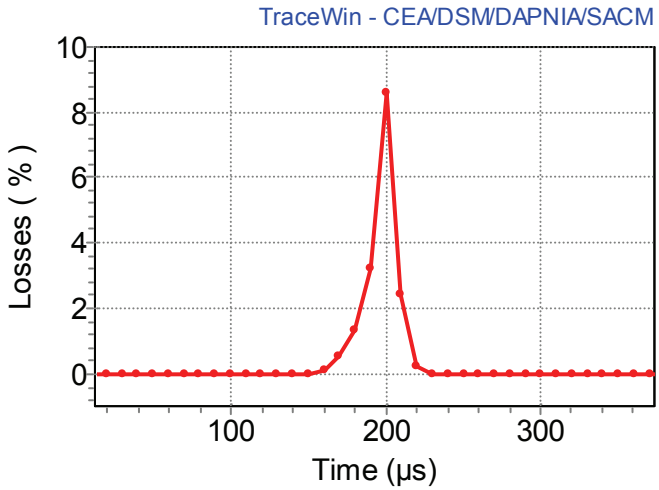

Figure 36 : Beam losses in function of time for T1=T2=200 µs

6 CONCLUSION

The present analysis demonstrates on the beam dynamics point of view that a fast retuning procedure can be envisaged without stopping the beam. This is what we called Scenario n°2.

Nevertheless, this Scenario n°2 implies stringent specifications, especially on:

- the fault detection time, that has to be extremely short (order of magnitude: 100 μs); this means that the RF control loop has to include some dedicated diagnostics and/or algorithms capable to detect (or anticipate) any RF malfunctioning and inform as quickly as possible the global feed-back system;
- the margins required on the accelerating field and RF power point of view, that are higher than in Scenario n°1 where the beam is stopped and the cavity detuned; this point could have some impact on the cost point of view.

Table 3 – Requirements and features of the 2 fault-recovery scenarios.

Scenario n°1 (stopping the beam)	Scenario n°2 (on-line)
- Implies a ≤ 1 sec beam stop	- No beam stop
-"Relatively fast" fault time detection	- "Extremely fast" fault time detection
- Lower margins / nb cavities required	- Higher margins / nb cavities required
- Small pre-defined set-points database	- Huge pre-defined set-points database
- Fast cold tuner management required	- Classical cold tuner management

Table 3 summarizes the main requirements and features for the two envisaged fault-recovery scenarios. Both scenarios are feasible on the beam dynamics point of view. The choice will first rely on the results of R&D activities to be performed on:

- fast RF fault detection
- fast cold tuning system management
- fast LLRF communication and data exchange

Once these points clarified, integrated reliability analysis and cost statements will have to be performed, so as to optimize the fault-recovery scenario process in terms of number of cavities involved, of accelerating field margins and of RF power budget.

REFERENCES

[1] H. Safa, A.C. Mueller, B. Carluec, “Requirements for the XADS accelerator and the technical answers”, PDS-XADS internal report, Deliverable 9, October 2002.

[2] J-L. Biarrotte, A.C. Mueller, B. Carluec, “Definition of the XADS-class reference accelerator concept & needed R&D”, PDS-XADS internal report, Deliverable 63, November 2004.

[3] J-L. Biarrotte et al., “A reference accelerator scheme for ADS applications”, Nuclear Instruments and Methods A 562 (2006) 565-661.

[4] J-L. Biarrotte, A.C. Mueller, “R&D activities around the EUROTRANS accelerator for ADS applications”, Proc. ICENES Conference, Istambul, June 2007.

[5] J-L. Biarrotte, M. Novati, P. Pierini, D. Uriot, “Beam dynamics studies for the fault tolerance assessment of the PDS-XADS linac design”, Proc. HPPA4 Workshop, Daejon, May 2004.

[6] J. Galambos et al., “Operational Experience of a Superconducting Cavity Fault Recovery System at the Spallation Neutron Source”, Proc. HPPA5 Workshop, Mol, May 2007.

[7] J. Galambos, personal communication.

[8] M. Luong et al., “RF control system modeling”, EUROTRANS internal report, Deliverable 1.40, June 2007.

[9] C. Joly et al., LLRF07 workshop, Knoxville, October 2007.

[10] T. Schilcher, “Vector sum control of pulsed accelerating fields in Lorentz force detuned superconducting cavities”, TESLA-report 98-20, Hamburg, 1998.

[11] J-L . Biarrotte, “Modélisation RF d’une cavité accélératrice supraconductrice”, IPNO report 07-06, Orsay, 2007.

[12] R. Duperrier, N. Pichoff, D. Uriot, “CEA Saclay codes review”, Proc. ICCS Conference, Amsterdam, April 2002.